A Theoretical Investigation of Excited-State Properties of the Adenine−Uracil Base Pair

M. K. Shukla and Jerzy Leszczynski*

Computational Center for Molecular Structure and Interactions, Department of Chemistry, Jackson State University, 1400 J.R. Lynch Street, Jackson, Mississippi 39217

Received: December 20, 2000; In Final Form: October 5, 2001

Molecular geometries of adenine−uracil (AU) base pair were optimized in the ground and selected low-lying singlet $\pi\pi^*$ and $n\pi^*$ excited states. The ground-state geometry optimized at the Hartree−Fock level of theory without symmetry restrictions was found to be planar; the predicted planarity was validated by harmonic vibrational frequency calculations. Excited states were generated employing the configuration interaction technique involving singly excited configurations (CIS method) using a ground-state-optimized geometry, and this was followed by excited-state geometry optimizations under planar symmetry. The 6-31++G(d,p) basis set was used in all calculations. The computed electronic transitions of adenine and uracil after linear scaling were found to be in good agreement with the corresponding experimental data. Electronic excitations were found to be localized at either of the monomeric units. It is predicted that among the states studied here the AU base pair has one charge transfer type singlet excited state lying slightly higher in energy. This state is characterized by the excitation of an electron from the occupied orbitals of the adenine moiety to the virtual orbitals of the uracil moiety. In the $S_4(\pi\pi^*)$ singlet excited state where the excitation is localized at the uracil moiety of the AU base pair, a large increase in the C′5−C′6 bond length of uracil is revealed. Such a large increase can account for the photophysical reactivity of pyrimidines in view of photodimerization. The base pair geometry is predicted to be largely destabilized under $n\pi^*$ excitations.

1. Introduction

The static and dynamic properties of polynucleotides demand a detailed knowledge of the structures of nucleic acid bases and related compounds not only in the ground state but also in different excited states. A continuous increment of UV exposure on earth due to ozone depletion is posing a dangerous challenge to the living world.[1] It is well-know that UV radiation can alter DNA by photostimulation and the subsequent formation of pyrimidine dimers.[2] Optical spectroscopic methods including UV absorption and emission, linear dichroism (LD), circular dichroism (CD), and magnetic circular dichroism (MCD) have been proven to be important tools for monitoring nucleic acid structural changes as well as for probing interactions of DNA and RNA with proteins and small molecules.[3] Absorption spectroscopy is one of the oldest and most commonly used techniques in chemical science to elucidate the structure. As the absorption is vertical, to analyze which wavelength would be absorbed the knowledge of the energy difference between the ground state and excited states lying vertically above the ground state is necessary. In the case of a fluorescence process, the knowledge of the relaxed singlet excited state is needed while for the explanation of phosphorescence the relaxed triplet state is necessary.

Many chemical processes proceed through photoactivation such as, for example, the electronic transfer process in photosynthesis, the charge transfer through antenna complexes, isomerization in bacteriorhodopsin, animal visual pigments, "retinol", the formation of twisted charge-transfer species, excited-state proton transfer, etc.[4] The starting point for explaining the excited states of polynucleotides should be the knowledge of excited states of the constituted purines and pyrimidines and their hydrogen-bonded dimers. In polynucleotides, the excited states might be influenced by the energy transfer between constituents, by hydrogen bonding with possible proton transfer in the excited state, or by changes of such intramolecular properties as nonradiative transition rates of intersystem crossing.[3a−e] Several rigorous and reliable vertical excitation energy calculations have been carried out on nucleic acid bases and their substituted analogues;[5] studies of the excited-state geometries are now also gaining momentum.[6]

The free DNA bases can occur in more than one tautomeric form.[3a,5a−d,7,8] The equilibrium between different tautomeric forms depends on the nature of the environment. The existence of more than one tautomeric form of many DNA bases complicates the analysis of the absorption and emission spectra, as the minor tautomers are also likely to contribute.[9] For example, in the case of adenine and guanine, the major part of fluorescence is attributed as being a result of emission from the N7H tautomer, while, in the case of 2-aminopurine, the participation of both N7H and N9H tautomers in the fluorescence emission is obtained.[3a,6e,9a,10] It is well-known that the quantum yield for fluorescence is very low for all DNA bases.[3a,c] It can be speculated that evolution has selected genetic material with poor luminescence and short-lived excited states to provide autoprotection from the photoreactions in living cells. However, it is interesting to note that two bases, adenine and 2-aminopurine, have an entirely different quantum yield. Thus, while the quantum yield for fluorescence is around 0.5 for 2-aminopurine, it is only about 0.0003 for adenine.[3a,11] On the basis of the ground and singlet excited-state geometry optimization studiy of adenine tautomers, the N7H form is found to undergo a large geometry change consequent to the relaxation of the $n\pi^*$ state.[6e,10] The final geometry resembles a twisted intramolecular charge transfer state, although only a small charge transfer was

* Corresponding author. E-mail: jerzy@ccmsi.jsums.edu.

10.1021/jp004551n CCC: $22.00 © 2002 American Chemical Society
Published on Web 01/22/2002

revealed.[6e,10] It has been suggested that both the N9H and N7H tautomers of 2-aminopurine contribute to the absorption and fluorescence spectra.[6e,10] In the case of adenine the N9H tautomer is present dominantly in the ground state in aqueous solution, but the fluorescence mainly originates from the N7H tautomer.[6e,9a,10] Furthermore, the fluorescence of 2-aminopurine is absorbed by its cation obtained by the protonation of the N7 site of the N9H tautomer, the fluorescence of which can have an anti-Stokes component.[10,12]

In this work, we have carried out a computational study of the RNA adenine−uracil (AU) base pair in the ground and selected singlet excited states. However, the real systems of nucleic acids in which stacking of bases and the surrounding environments play an important role are much more complex.[3a−e,6f,13] This study of the AU base pair sheds some light on the photophysical behavior of nucleic acids and is a step closer toward gaining an understanding of nucleic acid structures and properties not only in the ground state but also in the excited states.

2. Computational Details

Ground-state geometry of the AU base pair was optimized using the ab initio restricted Hartree−Fock method. The excited states were generated using the configuration interaction considering single electron excitations (CIS) from the filled to the unfilled molecular orbitals using the optimized ground-state geometry, and this was followed by geometry optimizations in different excited states. The standard 6-31++G(d,p) basis set was used in all calculations. The nature of the ground-state potential surface was analyzed by vibrational frequency calculations. Due to the large size of the system, the excited-state geometries were optimized under C_s symmetry. In the CIS calculation[14] all of the occupied and unoccupied orbitals were considered using the option CIS=FULL. All reported calculations were performed using the Gaussian 94 program.[15]

Theoretical investigations of different base pairs using the HF, MP2, and DFT methods employing various basis sets have shown that the HF method is reasonable in the computation of interaction energies and geometries.[16] The CIS method is the HF analogue for the excited-state calculations and is considered as the zeroth-order approximation for the study of excited-state potential energy surfaces.[14] It is well-known that CIS-computed transition energies are quite larger than the corresponding experimental transition energies, and linear scaling is needed to compare with experimental data.[5c,6a,c−e] The scaled CIS transition energies are found to be satisfactory in explaining experimental transitions of different varieties of molecules.[5c,6a,c−e,17]

There are no experimental techniques to determine directly the excited-state geometries of complex molecular systems such as purines, pyrimidines, and base-pair complexes. The supersonic jet cooled spectroscopic[18a] and resonance Raman[18b] studies of uracil and thymine have indicated the nonplanarity of the excited-state geometries. Excited-state geometry optimization studies of pyrimidines using the CIS method have also shown the nonplanar excited-state geometries.[6c] We believe that the application of the CIS method provides reasonably good data for AU base pair excited-state geometries.

The basis set superposition error (BSSE) corrected interaction energies in the ground and different excited states were computed using the Boys−Bernardi counterpoise correction schemes.[19] The interaction energy (E_{int}) in the ground state was calculated using the formula

$$E_{int} = E(\mathrm{AU}) - E(\mathrm{A_{AU}}) - E(\mathrm{U_{AU}}) \quad (1)$$

where E(AU) is the total energy of the AU base pair in the ground state and $E(\mathrm{A_{AU}})$ and $E(\mathrm{U_{AU}})$ are the total energies of the adenine and uracil moieties, respectively, within the framework of the optimized AU base pair geometry, while the ghost atoms were added in place of the complementary base of the complex. The interaction energy in the excited state ($E^{(n)}$int) where the excitation is localized at the adenine moiety was calculated using the formula

$$E^{(n)}\mathrm{int} = E^{(n)}(\mathrm{AU}) - E^{(n')}(\mathrm{A_{AU}}) - E^{(0')}(\mathrm{U_{AU}}) \quad (2)$$

whereas, for the state where excitation is localized at the uracil moiety, the interaction energy was calculated using the formula

$$E^{(n)}\mathrm{int} = E^{(n)}(\mathrm{AU}) - E^{(0)}(\mathrm{A_{AU}}) - E^{(n')}(\mathrm{U_{AU}}) \quad (3)$$

In eqs 2 and 3, $E^{(n)}$(AU) is the total energy of the AU base pair in the nth excited state and $E^{(n')}(\mathrm{A_{AU}})$ and $E^{(n')}(\mathrm{U_{AU}})$ are the total energies of the adenine and uracil moieties, respectively, in the n'th excited state which corresponds to the nth state of the AU base pair (since the nth state of the AU base pair may not necessarily correspond to the nth state of adenine or uracil; see Table 1). $E^{(0)}(\mathrm{A_{AU}})$ and $E^{(0)}(\mathrm{U_{AU}})$ are the ground-state total energies of the adenine and uracil moieties, respectively. In these calculations the geometries of adenine and uracil moieties are within the framework of the optimized geometry of the AU base pair in the nth excited state, while the ghost atoms are added in place of the complementary base of the complex.

3. Results and Discussion

The optimized geometry of the AU base pair (Figure 1) in the ground state is predicted to be planar at the HF/6-31++G(d,p) level. The predicted planarity was validated by the calculations of Hessians at the optimized geometry. To evaluate the geometrical deformation of individual monomers consequent to base pair formation, the geometries of individual bases (adenine and uracil) under the constraint of planarity were also optimized. The deformation energy calculated as the energy difference between the separately optimized isolated bases to those within the framework of the optimized base pair unit indicates that the geometrical deformation is negligible in going from individual bases to base pair; it is approximately 0.22 kcal/mol for adenine while approximately 0.34 kcal/mol for uracil.

3.1. Vertical Excitations. The 10 lowest vertical singlet excitation energies, oscillator strengths, and their assignments of the AU base pair are presented in Table 1. The vertical singlet excitation energies of individual constituents (adenine and uracil) of the AU base pair within the geometrical framework of the optimized complex are also presented in the same table. The transitions are characterized by the $\pi\sigma^*$, $\pi\pi^*$, or nπ^* types and are localized at the either of the bases. The only exception was found for the $S_9(\pi\pi^*)$ state discussed later (Table 1). In an experimental study of the AT, GC polymers and natural DNA bases, the electronic transitions were also assigned to the corresponding monomer bases.[20] Since the $\pi\pi^*$ and nπ^* transitions of nucleic acid bases are discussed in different experimental and theoretical publications,[3−6] we will, therefore, restrict our discussion to these important $\pi\pi^*$ and nπ^* types of transitions.

Before discussing the transitions of the AU base pair, it is imperative to discuss the transition energies of isolated bases to examine if they are in accordance with the corresponding

TABLE 1: Vertical Excitation Energies (Δ*E*, eV), Oscillator Strengths (*f*), and Their Assignments of the AU Base Pair and Their Constituent Bases (Adenine (A) and Uracil (U))[a]

AU base pair:[b] state(assgnt)/Δ*E* (*f*)	adenine: Δ*E* (*f*) (assgnt)	uracil: Δ*E* (*f*) (assgnt)
$S_1(\pi\sigma^*)$ 6.17 (0.0057) (A*)	6.19 (0.0074) ($\pi\sigma^*$)	
$S_2(\pi\pi^*)$ 6.41 (0.5106) (A*)	6.43 (0.4124) ($\pi\pi^*$)	
$S_3(\pi\pi^*)$ 6.51 (0.0253) (A*)	6.56 (0.0214) ($\pi\pi^*$)	
$S_4(\pi\pi^*)$ 6.66 (0.3576) (U*)		6.66 (0.4626) ($\pi\pi^*$)
$S_5(n\pi^*)$ 6.66 (0.0001) (U*)		6.42 (0.0000) ($n\pi^*$)
$S_6(\pi\sigma^*)$ 6.70 (0.0002) (A*)	6.59 (0.0002) ($\pi\sigma^*$)	
$S_7(\pi\sigma^*)$ 6.71 (0.0133) (U*)		6.74 (0.0135) ($\pi\sigma^*$)
$S_8(\pi\sigma^*)$ 6.97 (0.0043) (A*)	6.97 (0.0033) ($\pi\sigma^*$)	
$S_9(\pi\pi^*)$ 7.22 (0.0230) (A → U*)		
$S_{10}(n\pi^*)$ 7.29(0.0005) (A*)	7.13 (0.0005) ($n\pi^*$)	

[a] Geometries of A and U are within the framework of the optimized AU base-pair geometry. [b] A* and U* indicate that the corresponding moiety of the base pair is excited. A → U* indicates excitation from the adenine to the uracil moiety.

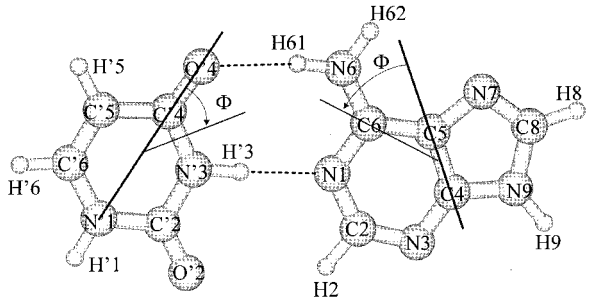

Figure 1. Atomic numbering schemes in the AU base pair. Φ shows the transition moment direction for individual bases according to Tinoco−DeVoe convention.

experimental data and other theoretical results. The low-lying singlet vertical $\pi\pi^*$ and $n\pi^*$ transition energies of adenine and uracil are presented in Table 2 along with CASPT2/CASSCF and some selected experimental results. It should be noted that the $\pi\sigma^*$ types of transitions were also found among these transitions which we are not presenting here. Furthermore, the geometries taken for the transition energy calculations are those within the framework of the optimized ground state AU base pair geometry and are within the error of 0.05 eV compared to transition energies obtained using individually optimized geometries. It is now well established that the main absorption band (near the 260 nm (4.77 eV) region) of adenine consists of two $\pi\pi^*$ transitions, one being stronger and short-axis polarized while the second is considerably weaker and is long-axis polarized.[3a,b] The relative positions of both transitions are environmentally dependent.[3a,b] In water solution the stronger band which appears at 261 nm (4.75 eV) is short-axis polarized and a weak band which appears as a shoulder near 267 nm (4.64 eV) is long-axis polarized.[3a,b] The absorption spectra of adenine in vapor phase exhibit only two peaks near 252 and 207 nm (4.92 and 4.99 eV, respectively).[21] The CIS-computed transition energies shown in Table 2 suggest that the first $\pi\pi^*$ transition

TABLE 2: Low-Lying Singlet $\pi\pi^*$ and $n\pi^*$ Vertical Excitation Energies (Δ*E*, eV), Oscillator Strengths (*f*), Transition Moment Directions (Φ, deg), and Dipole Moments (μ, D) of Adenine and Uracil[a]

CIS						exptl[d]			
Δ*E*	*f*	Φ	μ	Δ*E*[b]	CASPT2/CASSCF:[c] Δ*E*[1]/Δ*E*[2]/*f*/Φ/μ	abs	CD	cryst: Δ*E*/*f*/Φ	LD: Δ*E*/*f*/Φ
					Adenine: $\pi-\pi^*$ Transitions				
6.43	0.4124	56	2.03	4.63	5.13/5.73/0.07/23/2.37			4.51/0.1/83	4.55/0.047/66
6.56	0.0214	−42	3.72	4.72	5.20/6.48/0.37/37/2.30	4.92	4.68	4.68/0.2/25	4.81/0.24/19
7.28	0.0179	−51	1.53	5.24					5.38/0.0 27/−15
7.87	0.4854	−44	2.00	5.67	6.24/7.80/0.851/−7/2.13	5.99	5.77	5.82/0.25/−45	5.80/0.14/−21
8.26	0.3066	18	3.25	5.95					
				6.0[e]	6.72/8.30/0.159/40/4.60		6.36	6.08/0.11/15	5.99/0.12/−64
8.40	0.4368	−85	3.92	6.05					
					Adenine:$n-\pi^*$ Transitions				
7.13	0.0005		2.33	5.13	6.15/6.43/0.001/−/2.14				
7.57	0.0025		0.73	5.45	6.86/7.16/0.001/−/1.93				
					Uracil: $\pi-\pi^*$ Transitions				
6.66	0.4626	−7	5.13	4.80	5.00/6.88/0.19/−7/6.3	5.1	4.73	4.51/−/ −9	
8.24	0.0668	75	2.97	5.93					
				6.03[f]	5.82/7.03/0.08/−29/2. 4	6.0	5.77	5.82/−/ 59	
8.50	0.1481	53	4.68	6.12					
8.90	0.3615	−51	3.77	6.41	6.46/8.35/0.29/23/6.9	6.6	6.36		
9.55	0.2680	−26	2.91	6.88	7.00/8.47/0.76/−42/3. 7			7.00	
					Uracil: $n-\pi^*$ Transitions				
6.42	0.0		2.98	4.62	4.54/4.78/−/−/3.4				
7.86	0.0005		5.32	5.66	6.00/6.31/−/−/4.8				

[a] Geometries of A and U are within the framework of the optimized AU base-pair geometry. The DeVoe−Tinoco convention is used for the transition moment directions (see Figure 1 for explanation). The computed ground-state dipole moment for adenine is 2.53 and for uracil is 4.91 D. [b] Scaled (scaling factor 0.72) energy. [c] Δ*E*[1] corresponds to CASPT2 and Δ*E*[2] corresponds to CASSCF transition energies; for details, see ref 5d for adenine and ref 5f for uracil. For the oscillator strength of $n-\pi^*$ transitions of uracil, see ref 5f. [d] Abs: absorption in vapor phase (see ref 21). CD: CD spectra of base nucleotides in aqueous medium (see ref 22c). Crystal: results for adenine correspond to 9-methyladenine (see ref 24a), and those for uracil correspond to 1-methyluracil (see ref 28). LD: LD spectra of 9-methyladenine oriented in stretch poly(vinyl alcohol) film (see ref 3j). [e] Average of transitions at 5.95 and 6.05 eV. [f] Average of transitions at 5.93 and 6.12 eV.

is stronger, while the second is comparatively weaker. The energy difference between these two transitions is about 0.1 eV which is in agreement with the observed splitting of 0.11 eV of corresponding transitions of adenine obtained in an aqueous medium (Table 2).[3b] The computed dipole moments of these two states (Table 2) suggest that the second transition having larger dipole moment than the first transition will stabilize more in an aqueous medium. Consequently, under aqueous solvation, the first transition will have a lower intensity than the second transition. The data presented in Table 2 suggest that the computed scaled CIS transitions are in good agreement with the corresponding experimental values and the transitions obtained by the CASPT2 method.[5d] Although the transition energies obtained by the CASPT2 methods are slightly higher than the experimental data and the scaled CIS transition energies, the corresponding CASSCF values are much greater (Table 2).[5d] The first CASPT2 transition energy has a larger oscillator strength than the second transition suggesting that the CASPT2 results are closer to the aqueous solution results. The CIS calculation predicts a weak $\pi\pi^*$ transition near 5.24 eV which has not been found in the CASPT2 and CASSCF calculations.[5d] Although the existence of a transition near 230 nm (5.39 eV) has been predicted in earlier semiempirical calculations[3a] and indicated in the MCD[22a] and CD[22b,c] spectra, they have been assigned to the nπ^* type on the basis of the semiempirical prediction of an existence of the nπ^* transition in the same region.[3a] Recently Holmen et al.[3j] have found the existence of a weak $\pi\pi^*$ transition near 5.38 eV with an oscillator strength of 0.027 in the stretch film experiment on 9-methyladenine. Thus, our CIS-predicted transition near 5.24 eV is in agreement with the recent stretch film experimental result.[3j] The experimental transition near 6.0 eV (6.36 in CD, 6.08 eV in crystal, 5.99 eV in LD) is revealed to be a composite by the CIS method where the two nearby transitions near the 5.95 and 6.05 eV region (scaled values) are contributing to it (Table 2). This prediction is in accordance with the MCD results which suggest that the UV-absorption band near the 200 nm (6.2 eV) region is composed of two transitions and their transition moment directions are not parallel with each other.[23] With regard to the transition moment directions of adenine, different experimental methods give different directions, and their magnitudes are found to be dependent on the experimental environment.[3a,j,24] The transition dipole moment directions for adenine measured in crystal[24a] and stretch film[3j] experiments are presented in Table 2. Among the CIS-computed transition moment directions, some are found to be in agreement with the crystal results, while others are closer to the stretch film results (Table 2). Further, computed transition moment directions for the composite transitions near 5.95 and 6.05 eV are found to be 18 and -85°, respectively (Table 2). This prediction is in accordance with the earlier discussed MCD finding regarding the nonparallelism of transition moment directions.[23]

The existence of an nπ^* transition near 244 and 204 nm (5.08 and 6.08 eV) in 2′-deoxyadenosine has been tentatively assigned by Clark.[24b] Although the computed first nπ^* transition near 5.13 eV is close to the 244 nm (5.08 eV) prediction and about 0.2 eV lower than the CD[22b,c] and MCD[22a] results of adenine discussed earlier, the second nπ^* transition near 5.45 eV is largely away from the experimental 204 nm (6.08 eV) value (Table 2). It is well-known that the nπ^* transitions are blue shifted under a hydrogen-bonding environment.[3a,c,25] A comparison of the dipole moments of these two nπ^* transitions (Table 2) suggests that under a hydrogen-bonding environment, the second transition with an appreciably low dipole moment would be more blue-shifted compared to the first transition. Therefore, the discrepancy discussed above would be eliminated under hydrogen-bonding environments. Similar conclusions were made in earlier investigations also.[5d] Thus it appears that, near the 245 nm region, two transitions of the $\pi\pi^*$ and nπ^* types are present in adenine.

The CIS-computed transition energies of uracil presented in Table 2 show that in the gas phase the first vertical singlet excited state of uracil has nπ^* character. This is in accordance with experimental observations in which in the gas phase or in aprotic solvent uracil and thymine have an nπ^* state as the lowest singlet excited state.[3a,26] The first singlet nπ^* transition is localized at the C4O4 group, and the second is localized at the C2O2 group. Assignments of these transitions are in agreement with the MRCI, RPA,[27] and CASSCF/CASPT2 results.[5f] Further, there is sufficient experimental and theoretical evidence to suggest the existence of an nπ^* transition near 250 nm (4.96 eV) of uracil in aqueous medium, the relative position of which is solvent dependent.[3a,5f,22] An existence of a second nπ^* transition near 217 nm (5.71 eV) has been suggested in 1-methyluracil.[28] The CIS-computed first two singlet nπ^* transitions are predicted to be near 4.62 and 5.66 eV; the corresponding dipole moments are 2.98 and 5.32 D, respectively, while the ground-state dipole moment is predicted to be 4.91 D (Table 2). This suggests that under hydration or hydrogen bonding environments the first transition will be largely destabilized and, therefore, blue-shifted. The corresponding effect on the second nπ^* transition would be small. Under such conditions the computed nπ^* transitions will be in agreement with the corresponding experimental values observed near 4.96 and 5.71 eV.[3a,5f,22,28] The data shown in Table 2 suggest that the observed spectral transitions[21,22c] can be explained easily in terms of the CIS-computed and scaled singlet vertical $\pi\pi^*$ transition energies within an error of 0.2 eV. There is also good correspondence between the CIS-computed scaled $\pi\pi^*$ excitation energies and those of the CASPT2 $\pi\pi^*$ excitation energies (Table 2).[5f] The CIS calculation predicts the composite nature of the second experimental gas-phase transition observed near 6.0 eV; the computed transitions near 5.93 and 6.12 eV are contributing to it (Table 2). Since the dipole moment of the state corresponding to the transition near 6.12 eV is much larger than the state corresponding to the transition near 5.93 eV, the stabilization of these two transitions would be different under an aqueous environment. The higher energy transition will be stabilized more than the lower energy transition. Therefore, it is expected that under hydration both of these transitions will give rise to one single transition. The CIS-computed transition moment direction for the first transition is found to be -7° (Table 2). This prediction is in agreement with the experimental value of -9° suggested by Vovrous and Clark.[28] It is difficult to comment on the computed transition moment direction for the second transition. First, the predicted nature of the transition is complex, and second, different experiments have suggested different values. Novros and Clark[28] have suggested two transition moment directions, namely -53 or $+59^\circ$, and favor the latter as being consistent with the LD spectra of uracil.[29a] But, Anex et al.[29b] have suggested the value of -31°. Eaton and Lewis have estimated that polarization of bands I and II are approximately perpendicular to each other.[29c] Holmen et al.[29d] have found an angle of 35° for the second transition of 1,3-dimethyluracil.

Among the vertical transitions of the AU base pair, the lowest singlet $\pi\pi^*$ excitation (S_2) is characterized by an intense transition localized at the adenine moiety and is followed by a

weak $\pi\pi^*$ excitation (S_3) localized also at the adenine moiety (Table 1). Next the $\pi\pi^*$ excitation (S_4) is localized at the uracil moiety and especially at the C′5−C′6 bond, the transition intensity being slightly weaker than the $S_2(\pi\pi^*)$ excitation (Table 1). The lowest singlet nπ^* excitation of the AU base pair is the fifth transition (S_5) localized at the uracil moiety. It is assigned to the excitation of a lone-pair electron of the C′4−O′4 group of uracil. In an earlier study of uracil, the transition involving the excitation out of the O2 carbonyl oxygen lone pair was predicted to be higher in energy than the transition involving the excitation out of the O4 carbonyl oxygen lone pair.[27] It should be noted that the $S_4(\pi\pi^*)$ and S_5(nπ^*) excited states are having approximately similar excitation energies (Table 1). The next singlet nπ^* transition (S_{10}(nπ^*)) is localized at the adenine moiety and is characterized by the excitation of a nitrogen lone pair of the purine ring. The S_9 transition of the AU base pair is a special kind of the $\pi\pi^*$ type. In this transition, the excitation is taking place from the π-type occupied orbitals of the adenine moiety to the π^*-type virtual orbitals localized at the uracil moiety of the AU base pair. Therefore, this excitation can be characterized as a charge-transfer type transition, giving rise to a charge-transfer type of the excited state (S_9). An analysis of the ground and different $\pi\pi^*$ and nπ^* excited-state total Mulliken charges at the adenine moiety of the AU base pair reveals insignificant charge transfer in going from the ground state to the $S_9(\pi\pi^*)$ excited state. But it yields a trend for the charge-transfer type nature of the state. For other states ($\pi\pi^*$ and nπ^*), Mulliken charges are found to be approximately the same as in the ground state, while for $S_9(\pi\pi^*)$ the excited-state charge was reduced by about 0.014 au. A charge-transfer type state with little charge transfer is not unexpected in view of the N7H tautomer of adenine. This tautomer in the lowest singlet nπ^* excited state is found to be in resemblance to the twisted intramolecular charge transfer state (TICT).[4d−e,6e,10] The amino group is twisted, and the plane containing the amino group is approximately perpendicular to the plane of the ring under the geometrical relaxation of this state.[6e,10] The small charge transfer from the ring system to the amino group was revealed in this process (the twisting of the amino group).[6e]

A comparison of transition energies of the AU base pair to those of isolated monomers computed within the framework of the optimized base-pair geometry (Table 1) reveals that there is no significant change in the energies of the $\pi\pi^*$ excitations in going from isolated bases to the AU base pair, while the transition energies of nπ^* excitations are increased (blue-shifted) upon base pair formation (Table 1). Such an increase in the nπ^* transition energies is in accordance with the established fact that hydrogen bonding plays a role in the blue shift of the nπ^* transition.[3a,c,25] On the basis of these results (spectral shift) it can be speculated that the hydrogen bond strengths would be similar in the ground and $\pi\pi^*$ excited states while decreased in the nπ^* excited states. The oscillator strength of the first $\pi\pi^*$ transition of adenine is increased after complex formation (AU base pair), while, for the second $\pi\pi^*$ transition, it has an insignificant effect (Table 1). In the case of uracil, after complexation the oscillator strength of the first $\pi\pi^*$ transition is decreased (Table 1). Furthermore, while in uracil the first transition is predicted to be of the nπ^* type and second is of $\pi\pi^*$ type, after base-pair formation both transitions have same energy. Such effect can be attributed to the blue shift in the transition energy of nπ^* excitation after the AU base-pair formation.[3a,c,25] Experimentally, the lowest singlet excited state of uracil is predicted to be of the nπ^* type in an aprotic environment, while, in the protic environment, the nature of the lowest singlet excited state is changed to the $\pi\pi^*$ type.[3a,26] Thus, very weak coupling in $\pi\pi^*$ spectral transitions of individual bases is revealed after base-pair formation (Table 1).

TABLE 3: Ground- and Excited-State Optimized Bond Lengths (Å) and Bond Angles (deg) of the AU Base Pair

	S_0	$S_2(\pi\pi^*)$	$S_4(\pi\pi^*)$	S_5(nπ^*)	S_{10}(nπ^*)
			Bond Lengths		
N1−C2	1.334	1.323	1.332	1.337	1.379
C2−N3	1.311	1.389	1.311	1.311	1.370
N3−C4	1.332	1.284	1.332	1.330	1.315
C4−C5	1.375	1.428	1.375	1.376	1.380
C5−C6	1.405	1.457	1.405	1.401	1.446
N1−C6	1.335	1.322	1.336	1.329	1.290
C5−N7	1.382	1.316	1.382	1.382	1.367
N7−C8	1.282	1.343	1.282	1.282	1.280
C8−N9	1.371	1.370	1.371	1.371	1.388
C4−N9	1.361	1.379	1.361	1.361	1.353
C6−N6	1.333	1.330	1.332	1.341	1.345
N′1−C′2	1.375	1.375	1.399	1.367	1.374
C′2−N′3	1.366	1.368	1.354	1.362	1.368
N′3−C′4	1.379	1.378	1.403	1.413	1.381
C′4−C′5	1.461	1.460	1.419	1.439	1.461
C′5−C′6	1.332	1.333	1.457	1.334	1.332
N′1−C′6	1.369	1.368	1.344	1.399	1.369
C′2−O′2	1.198	1.196	1.197	1.204	1.196
C′4−O′4	1.204	1.206	1.223	1.274	1.203
			Bond Angles		
N1−C2−N3	128.3	126.5	128.4	127.9	113.6
C2−N3−C4	111.7	113.2	111.6	112.0	122.9
N3−C4−C5	126.6	126.6	126.6	126.5	122.9
C4−C5−C6	116.5	115.1	116.6	116.3	115.3
C5−C6−N1	117.6	118.0	117.6	118.1	117.9
C2−N1−C6	119.3	120.7	119.3	119.1	127.4
C4−C5−N7	110.9	112.3	110.9	111.0	110.5
C5−N7−C8	104.3	105.3	104.3	104.2	105.6
N7−C8−N9	113.4	111.9	113.4	113.5	112.2
C8−N9−C4	106.5	107.2	106.5	106.5	106.4
C5−C4−N9	104.9	103.3	104.9	104.8	105.3
N6−C6−C5	122.7	119.7	122.7	122.2	120.1
N′1−C′2−N′3	114.4	114.3	116.0	115.7	114.2
C′2−N′3−C′4	126.8	126.7	124.7	123.1	127.0
N′3−C′4−C′5	115.0	115.1	116.3	118.5	114.8
C′4−C′5−C′6	118.8	118.8	121.1	118.0	118.9
C′5−C′6−N′1	121.9	121.9	115.4	120.8	122.0
C′6−N′1−C′2	123.1	123.1	126.4	124.0	123.1
O′2−C′2−N′3	123.6	123.6	125.0	122.1	123.6
O′4−C′4−N′3	120.6	120.7	118.8	117.7	120.7

3.2. Excited-State Geometries. The geometries of the AU base pair were optimized for two singlet $\pi\pi^*$ (S_2 and S_4) and two singlet nπ^* (S_5 and S_{10}) excited states using the CIS method.[14] The selection of these states was based on the fact that they are the lowest singlet excited states of either the $\pi\pi^*$ or the nπ^* type localized on the adenine or uracil moieties under the AU base-pair excitations. Optimized bond lengths and bond angles (for heavy atoms) in these excited states along with the optimized ground-state parameters are presented in Table 3. From the ground state to the $S_2(\pi\pi^*)$ excited state, the geometry of the adenine moiety is significantly changed while the uracil geometry is intact (Table 3). The change in the geometry of adenine only is not unexpected as the excitation ($S_2(\pi\pi^*)$) is localized at this moiety. The most prominent changes are confined at the C2=N3−C4=C5−N7=C8 and C5−C6 fragments of adenine. The C2N3, C4C5, C5C6, and N7C8 bond lengths are increased between 0.05 and 0.08 Å, while the N3C4 and C5N7 bond lengths are decreased by about 0.048 and 0.066 Å, respectively, compared to the respective ground-state values (Table 3). Thus, the characteristics of single and double bonds in C2=N3−C4=C5−N7=C8 fragments are interchanged in the $S_2(\pi\pi^*)$ excited state. Interestingly, the C5−C6 bond length is

further increased by about 0.052 Å in this state. In a recent excited-state geometry optimization study of adenine, similar changes are predicted in the geometry of the lowest singlet $\pi\pi^*$ excited state of the N9H tautomer of the molecule.[10]

In the $S_4(\pi\pi^*)$ excited state, where the excitation is localized at the uracil moiety, the geometrical changes are also accompanied to the uracil. The geometry of adenine remains unchanged compared to the ground-state geometry (Table 3). As compared to the ground state, the alternate ring bond lengths of uracil are found to increase and decrease in this state. The most significant change is revealed at the C′5−C′6 bond which is increased by about 0.125 Å compared to the ground-state value (Table 3). The large increase in this bond length is in accordance with the fact that the excitation is localized mainly at this bond (C′5−C′6), as discussed earlier. The excitation of the uracil moiety and the subsequent large increase of C′5−C′6 bond length may play a significant role in the photodimerization of pyrimidines in DNA.[3a,c] Further, this increase in the C′5−C′6 bond length of uracil is in agreement with the experimental fact that two pyrimidine units of nucleic acid forms photodimers through this site.[3a,c] In an earlier theoretical study of excited states of different pyrimidines, the geometrical distortion in the $\pi\pi^*$ excited state of thymine and cytosine was found to be very large especially around the C5−C6 bond; the length of this bond is also increased appreciably, while uracil is shown to be dissociative along this bond in this excited state.[6d] The large increase in the C′5−C′6 bond length of uracil consequent to the singlet $\pi\pi^*$ excitation may be related to the photodimerization of pyrimidines in which the singlet excimer state is suggested as a precursor.[6f,30]

In the $S_5(n\pi^*)$ excited state, geometrical changes are localized mainly at the N′3C′4C′5 fragment and the C′4O′4 group of uracil. The N′3−C′4 bond length is increased, and the C′4−C′5 bond length is decreased by about 0.034 and 0.022 Å, respectively. The most significant change is predicted in the C′4−O′4 bond which is increased by about 0.07 Å. Similar changes are found in an earlier study of the lowest singlet $n\pi^*$ excited state of uracil, but the geometry was also predicted to be nonplanar.[6d] However, it should be mentioned that this study has been performed under C_s symmetry in the excited state while earlier investigation was carried out without any symmetry restrictions.[6d]

In a comparison of the ground state to the $S_{10}(n\pi^*)$ excited state, significant changes are localized mainly at the N3=C2−N1=C6−C5 fragment of adenine. The N1−C6 bond length is decreased by about 0.045 Å, while N1C2, C2N3, and C5C6 bond lengths are increased by about 0.045, 0.059, and 0.041 Å, respectively. An appreciable change in bond angles is also revealed in this state; the N1−C2−N3 bond angle is decreased by about 14.7°, while the C2−N3−C4 and C2−N1−C6 bond angles are increased by 11.2 and 8.1°, respectively (Table 3).

Several attempts were made to optimize the $S_9(\pi\pi^*)$ charge-transfer type excited state of the base pair, but in all attempts optimizations were found to converge to the geometry of the $S_4(\pi\pi^*)$ excited state. As discussed earlier, this state ($S_4(\pi\pi^*)$) is characterized by the localization of the $\pi\pi^*$ excitation at the C′5−C′6 bond of the uracil moiety.

3.3. Hydrogen Bonding, Interaction Energies, and Dipole Moments. It is well-known that the AU base pair is characterized by the two hydrogen bonds. One of them is formed between the amino group hydrogen of adenine which acts as a hydrogen bond donor, and the C′4O′4 group of uracil acts as a hydrogen bond acceptor. The second bond is formed between, the N1 atomic site of adenine acting as a hydrogen bond acceptor and the N′3H site of uracil acting as a hydrogen bond donor (Figure 1). The formation of the third type of hydrogen bond between the C2H site of adenine and the C′2O′2 group of uracil has been speculated by Leonard et al.[31a] and supported by Starikov and Steiner.[31b] This third hydrogen bond is suggested to contribute to the stability of the AU base pair.[31a] However, theoretical calculations at the MP2 level do not support the existence of this type of hydrogen bond in the AU base pair.[32] Computed hydrogen bond distances and hydrogen bond angles are shown in Table 4. This table suggests that the N1···H′3 hydrogen bond is approximately linear (within 6°) in the ground and different excited states, while the O′4···H61 hydrogen bond deviates from linearity; the deviation is maximum in the $S_5(n\pi^*)$ excited state. In the $S_5(n\pi^*)$ excited state, the O′4−H61−N6 hydrogen bond angle is predicted to be about 162°. Further, in this state ($S_5(n\pi^*)$) the O′4···H61 hydrogen bond distance (and subsequently the O′4···N6 distance) is increased appreciably by about 0.7 Å, while the H′3···N1 hydrogen bond distance (and subsequently the N′3−N1 distance) is increased by about 0.07 Å. These changes can be accounted for the large increase in the C′4−O′4 bond length in this state (Table 3) and also for the fact that hydrogen-bonding interactions are destabilized in the $n\pi^*$ state.[33] In the S_2 and S_4 $\pi\pi^*$ excited states, the O′4···H61 hydrogen bond distance (and subsequently the O′4−N6 distance) are slightly decreased, while the H′3···N1 hydrogen bond distance (and subsequently the N′3−N1 distance) are slightly increased compared to the respective ground-state values (Table 4). In the $S_{10}(n\pi^*)$ excited state, the H′3···N1 hydrogen bond distance (and subsequently the N′3−N1 distance) is increased by about 0.14 Å, while no significant increase is found in the O′4···H61 hydrogen bond distance (Table 4). Thus, these results suggest that hydrogen bonding is destabilized under $n\pi^*$ excitations. A recent experimental study of the hydrated clusters of adenine in a supersonic molecular beam shows the weakening of hydrogen bonding and the subsequent fragmentation of adenine monomer hydrated clusters in the $n\pi^*$ excited state of adenine.[33] Del Bene[34] has also postulated the destablization of hydrogen bond in hydrated adenine clusters under $n\pi^*$ excitation. Krishna and Goodman[35] have found that the hydrogen bond for pyrazine and pyrimidine is very weak or does not even exist in the triplet $n\pi^*$ state. The hydrogen bonding of diazine in methanol or water is reported to be dissociative in the singlet $n\pi^*$ state.[36]

TABLE 4: Hydrogen Bond Lengths (Å) and Bond Angles (deg) of the AU Base Pair in the Ground and Different Excited States and Ground- and Excited-State Interaction Energies (E_{Int}, kcal/mol)

	states				
params	S_0	$S_2(\pi\pi^*)$	$S_4(\pi\pi^*)$	$S_5(n\pi^*)$	$S_{10}(n\pi^*)$
O′4···N6	3.082	3.011	3.029	3.742	3.092
N′3···N1	3.019	3.066	3.022	3.087	3.146
O′4···H61	2.088	2.016	2.032	2.786	2.104
H′3···N1	2.007	2.059	2.010	2.083	2.143
O′4−H61−N6	172.6	171.0	174.2	161.9	170.2
N′3−H′3−N1	177.6	174.6	177.0	183.0	174.1
E_{int}	−10.1	−10.2	−10.7	−5.9	−7.3

The computed interaction energies shown in Table 4 reveal that the complex is characterized by low interaction energy. Furthermore, the ground and $\pi\pi^*$ excited-state interaction energies are predicted to be similar, while in the $n\pi^*$ excited states the interaction energies (in magnitude) are found to be significantly reduced (Table 4). Thus, the AU base pair would be the least stable in the $S_5(n\pi^*)$ excited state where the excitation is localized at the C′4O′4 carbonyl group of the uracil moiety. Our speculation that the base pair would have similar

TABLE 5: Dipole Moment (μ, D) of the AU Base Pair in the Ground and Different Singlet Vertical $\pi\pi^*$ and nπ^* Excited States and Dipole Moment for Bases in the Ground State and Corresponding Excited States with Dipole Moments of the Geometrically Relaxed Excited States in Parentheses

AU base pair			
state(assgnt)	μ	adenine: μ	uracil: μ
S_0	2.22	2.53	4.91
$S_2(\pi\pi^*)$	3.03 (3.47)	2.03	
$S_3(\pi\pi^*)$	1.75	3.72	
$S_4(\pi\pi^*)$	2.49 (2.50)		5.13
$S_5(n\pi^*)$	2.58 (2.03)		2.98
$S_9(\pi\pi^*)$	4.68		
$S_{10}(n\pi^*)$	2.13 (2.29)	2.33	

stability in the ground and different singlet $\pi\pi^*$ excited states and reduced stability in the singlet nπ^* excited states is validated by interaction energy calculations. The computed interaction energy also supports the predicted weak coupling of the singlet $\pi\pi^*$ transitions of the individual bases after complex (the AU base pair) formation. Therefore, our prediction regarding the destabilization of the base pair in the nπ^* excited state is also validated from the interaction energy calculation and is in accordance with the different experimental results discussed above.

Ground and different vertical and relaxed singlet excited-state dipole moments of the AU base pair are presented in Table 5. For the sake of comparison, the dipole moments of the related states of constituent bases are also presented in Table 5. The computed ground-state dipole moment (2.53 D) of adenine is in agreement with the experimental value of 2.4 D for 9-methyladenine measured in a crystal environment[37a] and slightly lower than the measured dipole moment of 3.0 ± 0.2 D for 9-butyladenine in solution.[37b] The ground-state dipole moment of uracil is computed to be 4.91 D. The observed dipole moment for uracil using the microwave spectroscopic method[38a] is found to be 3.87 D while in a dioxane solution[38b] is found to be 4.16 D. The computed dipole moment at the CASSCF/CASPT2 level[5f] is found to be 4.4 D. Therefore, our computed dipole moment is closer to those observed in a dioxane solution. From the ground state to the first singlet $\pi\pi^*$ excited state of uracil, the computed dipole moment is increased (Table 2). The dipole moment of thymine (5-methyluracil) has been found to increase experimentally consequent to excitation.[39] The experimentally determined dipole moment for the first singlet $\pi\pi^*$ excited state of thymine is found to be 5.3 D.[39] The predicted dipole moment is in agreement with the CIS-computed dipole moment of the lowest singlet $\pi\pi^*$ transition of uracil (Tables 2 and 5). Table 5 suggests that the AU complex has the lowest dipole moment in the $S_3(\pi\pi^*)$ excited state and the highest in the $S_9(\pi\pi^*)$ singlet excited state. The dipole moments for those states where the excitation is localized at the adenine moiety are increased under geometrical relaxation, while in the $S_5(n\pi^*)$ excited state it is decreased after geometrical relaxation. The significantly large dipole moment of the $S_9(\pi\pi^*)$ excited-state further supports the charge-transfer nature of this state.

4. Conclusions

The computed excitation energies of adenine and uracil bases are in agreement with the corresponding experimental transitions. The predicted weak $\pi\pi^*$ transition near 5.38 eV in a recent experimental study of 9-methyladenine is also supported by this study. The electronic transitions of the AU base pair are found to localize at either of the monomeric units. From individual bases to the base pair complex, the nπ^* transitions are blue shifted while no appreciable change is found in the $\pi\pi^*$ transitions. The changes in the excited-state geometries are found to be similar to those under individual bases. It is found that the AU base pair has at least one charge-transfer type singlet $\pi\pi^*$ excited state lying slightly higher in energy and is characterized by the excitation of electrons from the occupied orbitals of the adenine moiety to the virtual orbitals of the uracil moiety. In the $S_4(\pi\pi^*)$ singlet excited state, where the excitation is localized at the uracil moiety of the AU base pair, a large increase in the C′5−C′6 bond length of uracil is revealed. Such an increase is important for the photophysical reactivity of pyrimidines in view of photodimerization. The interaction energy calculations suggest that the AU base pair is characterized by low interaction energy in the ground and excited states. It has a similar magnitude in the ground and different singlet $\pi\pi^*$ excited states and a significantly reduced magnitude in the singlet nπ^* excited states. The AU base pair is predicted to be largely destabilized in the nπ^* excited state.

Acknowledgment. The authors are thankful to NIH-RCMI Grant No. G1 2RR13459-21, NSF-CREST Grant No. 9805465, and ONR Grant No. N00014-98-1-0592 for financial assistance. The authors are also thankful to Prof. E. D. Jemmis, Department of Chemistry, University of Hyderabad, Hyderabad, India, and Prof. A. Sadlej, Department of Chemistry, Nicolaus Copernicus University, Torun, Poland, for fruitful discussions and suggestions.

References and Notes

(1) (a) Kerr, R. A. *Science* **1998**, *280*, 202. (b) Baird, C. *Environmental Chemistry*; W. H. Freeman and Co.: New York, 1995.

(2) (a) Darnell, J.; Lodish, H.; Baltimore, D. *Molecular Cell Biology*; Scientific American Books: New York, 1986; p 553. (b) Taylor, J.-S. *Chem. Educ*. **1990**, *67*, 835.

(3) (a) Callis, P. R. *Annu. Rev. Phys. Chem.* **1983**, *34*, 329. (b) Stewart, R. F.; Davidson N. *J. Am. Chem. Soc*. **1963**, *39*, 255. (c) Eisinger, J.; Lamola, A. A. In *Excited State of Proteins and Nucleic Acids*; Steiner R. F., Weinryb, I., Eds.; Plenum Press: New York, London, 1971. (d) Georghiou, S.; Gerke, L. S. *Photochem. Photobiol* **1999**, *69*, 646. (e) Rahn, R. O.; Yamane, T.; Eisinger, J.; Longworth, J. W.; Shulman, R. G. *J. Chem. Phys*. **1966**, *45*, 2947. (f) Ge, G.; Georghiou, S. *Photochem. Photobiol*. **1991**, *54*, 477. (g) Holmen, A.; Norden, B.; Albinson, B. *J. Am. Chem. Soc*. **1997**, *119*, 3114. (h) Michl, J. *Tetrahedron* **1984**, *40*, 3845. (i) Morgan, J. P.; Daniels, M. *Photochem. Photobiol*. **1980**, *31*, 101. (j) Holmen, A.; Broo, A.; Albinsson, B.; Norden, B. *J. Am. Chem. Soc*. **1997**, *119*, 12240.

(4) (a) Molteni, C.; Frank, I.; Parrinello, M. *J. Am. Chem. Soc*. **1999**, *121*, 12177. (b) Proppe, B.; Merchan, M.; Serrano-Andres, L. *J. Phys. Chem. A* **2000**, *104*, 1608. (c) Merchan, M.; Serrano-Andres, L.; Gonzalez-Luque, R.; Roos, B. O.; Rubio, M. *J. Mol. Struct. (THEOCHEM)* **1998**, *463*, 201. (d) Andreasson, J.; Holmen, A.; Albinsson, B. *J. Phys. Chem. B* **1999**, *103*, 9782. (e) Albinson, B. *J. Am. Chem. Soc*. **1997**, *119*, 6369. (f) Scheiner, S. *J. Phys. Chem. A* **2000**, *104*, 5898.

(5) (a) Callis, P. R. *Photochem. Photobiol*. **1986**, *44*, 315. (b) Borin, A. C.; Serrano-Andres, L.; Fulscher, M. P.; Roos, B. O. *J. Phys. Chem. A* **1999**, *103*, 1838. (c) Broo, A.; Holmen, A. *J. Phys. Chem. A* **1997**, *101*, 3589. (d) Fulscher, M. P.; Serrano-Andres, L.; Roos, B. O. *J. Am. Chem. Soc*. **1997**, *119*, 6168. (e) Fulscher, M. P.; Roos, B. O. J. *Am. Chem. Soc*. **1995**, *117*, 2089. (f) Lorentzon, J.; Fulscher, M. P.; Roos, B. O. *J. Am. Chem. Soc*. **1995**, *117*, 9265. (g) Shukla, M. K.; Mishra, P. C. *J. Mol. Struct*. **1994**, *324*, 241. (h) Shukla M. K.; Mishra, P. C. *J. Mol. Struct*. **1996**, *377*, 247. (i) Petke, J. D.; Maggiora, G. M.; Christoffersen, R. E. *J. Am. Chem. Soc*. **1990**, *112*, 5452.

(6) (a) Shukla, M. K.; Leszczynski, J. *Int. J. Quantum Chem*. **2000**, *77*, 240. (b) Mishra, P. C.; Jug, K. *J. Mol. Struct. (THEOCHEM)* **1994**, *305*, 139. (c) Shukla, M. K.; Mishra, P. C. *Chem. Phys*. **1998**, *230*, 187. (d) Shukla, M. K.; Mishra, P. C. *Chem. Phys.* **1999**, *240*, 319. (e) Broo, A. *J. Phys. Chem. A* **1998**, *102*, 526. (f) Danilov, V. I.; Slyusarchuk, O. N.; Alderfer, J. L.; Stewart, J. J. P.; Callis, P. R. *Photochem. Photobiol*. **1994**, *59*, 125. (g) Slater, L. S.; Callis, P. R. *J. Phys. Chem*. **1995**, *99*, 8572. (h) Fang, W.-H. *J. Chem. Phys*. **1999**, *111*, 5361.

(7) (a) Leszczynski, J. *J. Phys. Chem. A* **1998**, *102*, 2357. (b) Gorb, L.; Leszczynski, J. *J. Am. Chem. Soc*. **1998**, *120*, 5024. (c) Gorb, L.;

Leszczynski, J. *Int. J. Quantum Chem.* **1998**, *70*, 855. (d) Hobza, P.; Sponer, J. *Chem. Rev.* **1999**, *99*, 3247.

(8) (a) Leszczynski, J. In *Advances in Molecular Structure Research*; Hargittai, M., Hargittai, I., Eds.; JAI Press: Stamford, CT, 2000; Vol. 6, p 209. (b) Gorb, L.; Leszczynski, J. In *Computational Molecular Biology, Theoretical and Computational Chemistry Book Series*; Leszczynski, J., Ed.; Elsevier: Amsterdam, 1999; Vol. 8, p 167. (c) Sponer, J.; Hobza, P.; Leszczynski, J. In *Computational Molecular Biology, Theoretical and Computational Chemistry Book Series*; Leszczynski, J., Ed.; Elsevier: Amsterdam, 1999; Vol. 8, p 85. (d) Leszczynski, J. In *The Encyclopedia of Computational Chemistry*; John Wiley & Sons: New York, 1998; Vol. V, p 2951.

(9) (a) Wilson, R. W.; Callis, P. R. *Photochem. Photobiol.* **1980**, *31*, 323. (b) Dreyfus, M.; Dodin, G.; Bensaude, O.; Dubois, J. E. *J. Am. Chem. Soc.* **1975**, *97*, 2369. (c) Chenon, M. T.; Pugmire, R. S.; Grant, D. M.; Panzica, R. P.; Townsend, L. B. J. *Am. Chem. Soc.* **1975**, *97*, 4636. (d) Wilson, R. W.; Callis, P. R. *J. Phys. Chem.* **1976**, *80*, 2280. (e) Alyoubi, A. O.; Hilal, R. H. *Biophys. Chem.* **1995**, *55*, 231. (f) Mishra, P. C. *J. Mol. Struct.* **1989**, *195*, 201. (g) Santhosh, C.; Mishra, P. C. *J. Mol. Struct.* **1989**, *198*, 327.

(10) Mishra, S. K.; Shukla, M. K.; Mishra, P. C. *Spectrochim. Acta* **2000**, *56A*, 1355.

(11) Fletcher, A. N. *J. Mol. Spectrosc.* **1967**, *23*, 221.

(12) Santhosh, C.; Mishra, P. C. *Spectrochim. Acta* **1991**, *47A*, 1685.

(13) (a) Sponer, J.; Hobza, P.; Leszczynski, J. In *Computational Chemistry: Reviews of Current Trends*; Leszczynski, J., Ed.; World Scientific: Singapore, 2000; Vol. 5, p 171. (b) Sponer, J.; Leszczynski, J.; Hobza, P. *J. Phys. Chem. A* **1997**, *101*, 9489. (c) Sponer, J.; Gabb, H. A.; Leszczynski, J.; Hobza, P. *Biophys. J.* **1997**, *73*, 76. (d) Sponer, J.; Leszczynski, J.; Hobza, P. *J. Biomol. Struct. Dyn.* **1996**, *14*, 117. (e) Sponer, J.; Berger, I.; Spackova, N.; Leszczynski, J.; Hobza, P. *J. Biomol. Struct. Dyn. (Conversation 11)* **2000**, *2*, 383.

(14) Foresman, J. B.; Head-Gordon, M.; Pople, J. A.; Frisch, M. J. *J. Phys. Chem.* **1992**, *96*, 135.

(15) Frisch, M. J.; Trucks, G. W.; Schlegel, H. B.; Gill, P. M. W.; Johnson, B. G.; Robb, M. A.; Cheeseman, J. R.; Keith, T.; Petersson, G. A.; Montgomery, J. A.; Raghavachari, K.; Al-Laham, M. A.; Zakrzewski, V. G.; Ortiz, J. V.; Foresman, J. B.; Cioslowski, J.; Stefanov, B. B.; Nanayakkara, A.; Challacombe, M.; Peng, C. Y.; Ayala, P. Y.; Chen, W.; Wong, M. W.; Andres, J. L.; Replogle, E. S.; Gomperts, R.; Martin, R. L.; Fox, D. J.; Binkley, J. S.; Defrees, D. J.; Baker, J.; Stewart, J. P.; Head-Gordon, M.; Gonzalez, C.; Pople, J. A. *Gaussian 94, Revision E.2*; Gaussian, Inc.: Pittsburgh, PA, 1995.

(16) (a) Sponer, J. and Hobza, P. *J. Phys. Chem. A* **2000**, *104*, 4592. (b) Hobza, P.; Sponer, J.; Cubero, E.; Orozco, M.; Luque, F. J. *J. Phys. Chem. B* **2000**, *104*, 6286. (c) Kawahara, S.-I. And Uchimaru, T. *Phys. Chem. Chem. Phys.* **2000**, *2*, 2869. (d) Kawahara, S.-I.; Wada, T.; Kawauchi, S.; Uchimaru, T.; Sekine, M. *J. Phys. Chem. A* **1999**, *103*, 8516.

(17) (a) Organero, J. A.; Diaz, A. V.; Moreno, M.; Santos, L.; Douhal A. *J. Phys. Chem. A* **2001**, *105*, 7317. (b) Organero, J. A.; Moreno, M.; Santos, L.; Lluch, J. M.; Douhal, A. *J. Phys. Chem. A* **2000**, *104*, 8424. (c) Yamamoto, S.; Diercksen, G. H. F.; Karelson, M. *Chem. Phys. Lett.* **2000**, *318*, 590. (d) Nishimura, Y.; Tsuji, T.; Sekiya, H. *J. Phys. Chem. A* **2001**, *105*, 7273.

(18) (a) Brady, B. B.; Peteanu, L. A.; Levy, D. H. *Chem. Phys. Lett.* **1988**, *147*, 538. (b) Chinsky, L.; Laigle, A.; Peticolas, L.; Turpin, P.-Y. *J. Chem. Phys.* **1982**, *76*, 1.

(19) Boys, S. F.; Bernardi, F. *Mol. Phys.* **1970**, *19*, 553

(20) Chou, P.-J.; Johnson, W. C., Jr. *J. Am. Chem. Soc.* **1993**, *115*, 1205.

(21) Clark, L. B.; Peschel, G. G.; Tinoco, I., Jr. *J. Phys. Chem.* **1965**, *69*, 3615.

(22) (a) Voelter, W.; Records, R.; Bunnenburg, E.; Djerassi, C. *J. Am. Chem. Soc.* **1968**, *90*, 6113. (b) Brunner, W. C.; Maestre, M. F. *Biopolymers* **1975**, *14*, 555. (c) Sprecher, C. A.; Johnson, W. C., Jr. *Biopolymers* **1977**, *16*, 2243.

(23) Sutherland, J. C.; Griffin, K. *Biopolymers* **1984**, *23*, 2715.

(24) (a) Clark, L. B. *J. Phys. Chem.* **1990**, *94*, 2873. (b) Clark, L. B. *J. Phys. Chem.* **1995**, *99*, 4466.

(25) Brealey, G. J.; Kasha, M. *J. Am. Chem. Soc.* **1955**, *77*, 4462.

(26) Backer, R. S.; Kogan, G. *Photochem. Photobiol.* **1980**, *31*, 5.

(27) Petke, J. D.; Maggiora, G. M.; Christoffersen, R. E. *J. Phys. Chem.* **1992**, *96*, 6992.

(28) Novros, J. S.; Clark, L. B. *J. Phys. Chem.* **1986**, *90*, 5666.

(29) (a) Matsuoks, Y.; Norden, B. *J. Phys. Chem.* **1982**, *86*, 1378. (b) Anex, B. G.; Fucaloro, A. F.; Durra-Ahmed, J. *J. Phys. Chem.* **1975**, *79*, 2636. (c) Eaton, W. A.; Lewis, T. P. *J. Chem. Phys.* **1970**, *53*, 2164. (d) Holmen, A.; Broo, A.; Albinsson, B. *J. Phys. Chem.* **1994**, *98*, 4998.

(30) (a) Lamola, A. A. *Photochem. Photobiol.* **1968**, 7, 619. (b) Lisewski, R.; Wierzchowski, W. L. *Chem Commun.* **1969**, 348. (c) Fisher, G. I.; Johns H. E. *Photochem. Photobiol.* **1970**, *11*, 429.

(31) (a) Leonard, G. A.; McAuley-Hecht, Brown, T.; Hunter, W. N. *Acta Crystallogr.* **1995**, *51D*, 136. (b) Starikov, E. B.; Steiner, T. *Acta Crystallogr.* **1997**, *53D*, 345.

(32) Hobza, P.; Sponer, J.; Cubero, E.; Orozco, M.; Luque, F. J. *J. Phys. Chem. B* **2000**, *104*, 6286.

(33) Kim, N. J.; Kang, H.; Jeong G.; Kim, Y. S.; Lee, K. T.; Kim, S. K. *J. Phys. Chem. A* **2000**, *104*, 6552.

(34) Del Bene, J. E. *J. Mol. Struct.* **1984**, *108*, 179.

(35) Krishna, V. G.; Goodman, L. *J. Am. Chem. Soc.* **1961**, *83*, 2042.

(36) Baba, H.; Goodman, L.; Valenti, P. C. *J. Am. Chem. Soc.* **1966**, *88*, 5410.

(37) (a) Eisenstein, M. *Acta Crystallogr.* **1988**, *B44*, 412. (b) DeVoe, H.; Tinoco, I., Jr. *J. Mol. Biol.* **1962**, *4*, 500.

(38) (a) Brown, R. D.; Godfrey, P. D.; McNaughton D.; Pierlot, A. P. *J. Am. Chem. Soc.* **1988**, *110*, 2329. (b) Kulakowski, I.; Geller, M.; Lesyng, B.; Weirzchowski, K. L. *Biochim. Biophys. Acta* **1974**, *361*, 119.

(39) Liptay, W. In *Excited States*; Lim, E. C., Ed.; Academic Press: New York, 1974; Vol. 1, p 129.